ECS Transactions, 16 (35) 163-169 (2009)
10.1149/1.3123137 ©The Electrochemical Society

Charge Transfer and Charge-Discharge Kinetics in Lithium-ion Batteries

T. Richard Jow[a], Jan L. Allen[a], Bridget Deveney[b], Kamen Nechev[b]

[a] Army Research Laboratory, 2800 Powder Mill Road, Adelphi, Maryland 20783, USA
[b] Saft America, Inc., 107 Beaver Court, Cockeysville, Maryland 21030, USA

Charge transfer and charge-discharge kinetics of practical Li-ion cells were investigated using AC impedance and DC pulse methods. Preliminary AC impedance results indicated that the activation energy for charge transfer for high power Li-ion cells employing carbonate-linear ester solvent mixtures was similar to that for cells employing carbonate solvents as reported before. At 100 milliseconds (ms), the pulsed DC impedance indicated that the charge and discharge kinetics were fast and at about the same rate. At 15 seconds (s), the pulsed DC charge resistance was apparently higher than the discharge resistance especially at temperatures below –20 ^{o}C. The slower charging kinetics may be limited by the desolvation and electron transfer steps relating to solid-electrolyte interface influenced Li^{+} intercalation into the carbonaceous anode and possibly Li diffusion in the carbonaceous anode.

Introduction

Li-ion batteries capable of high rate charge and discharge in wide temperature range with long storage and cycle life are increasingly needed for various applications including power tools and hybrid/plug-in hybrid electric vehicles (HEV/PHEV). To improve the rate performance, the following strategies are often taken:

1. Reduce particle size or increase surface area of active materials,
2. Lower electronic resistance including contact resistance between electrode materials and current collectors and between current collectors and cell case, particle and particle contact resistance within electrodes, and
3. Increase conductivity of electrolytes especially at low temperatures.

These strategies are quite effective in improving the rate considering the various charge transfer processes involved in charging and discharging a cell.

Reducing the particle size essentially reduces the distance that Li travels within the active materials and increases the area for Li^{+} reduction and Li dissolution. This results in higher discharge/charge rate and utilization of the active materials. Lower electronic resistance reduces the IR voltage loss in the circuit and thus increases discharging voltage and reduces charging voltage for higher charging efficiency. Increased electrolyte conductivity will increase the rate of supplying Li^{+} to the reactive surfaces and also reduce the overall resistance of the cell. The questions are whether these improvements are sufficient at lower temperatures or at sustained high rate operations.

The existence of solid-electrolyte interface (SEI) on the electrode surfaces and the fact that the Li^{+} is moving in a solvated state in the nonaqueous electrolytes affect the charge/discharge kinetics. Furthermore, the diffusion of Li in the active materials that

affect the amount of Li that can be diffused to or away from the interface could also play a role in the charge/discharge kinetics especially at high rates[1].

For example, during charge of the cell, two major processes are happening. The first, at the positive electrode side, is a dissolution (or ionization of Li) at the interface of the positive electrode and the "solid electrolyte interface (SEI)" layer, which was formed on the surface of the electrode when the cell was initially formed. This process produces Li^+, which transports across the SEI layer, and an electron that travels through the electron conducting network within electrode and reaches the current collector to the outside. The Li^+ is then transported to the negative electrode, in a solvated form, as represented by "Li^+". The steps can be expressed below.

$$LiMO_2 \xrightarrow{Dissolution} Li_{1-x}MO_2 + x\ Li^+ + x\ e^- \quad (1)$$

$$Li^+ \xrightarrow{Solvation} \text{“}Li^+\text{”} \quad (2)$$

The second, at the negative electrode side, is the desolvation of "Li^+", which sheds the solvated solvent molecules before transporting through the SEI, which was formed on the negative electrode when the cell was initially formed. At the negative electrode surface, Li^+ takes an electron and forms Li, which intercalates into the anode. The key steps can be expressed as the following.

$$\text{“}Li^+\text{”} \xrightarrow{Desolvation} Li^+ \quad (3)$$

$$Li_{1-y}C_6 + x\ Li^+ + x\ e^- \xrightarrow{ElectronTransfer} Li_{x+1-y}C_6$$

$$(\text{or } x\ Li^+ + x\ e^- \xrightarrow{ElectronTransfer} x\ Li\ ) \quad (4)$$

During discharge, the steps are reversed with respect to the charging process. Which step is limiting in the charge or discharge process has been a subject of interest for improving the rate performance. Recently, Ogumi and his group[2-6] at Kyoto University have made extensive studies on Li^+ interfacial charge transfer kinetics and have identified that the de-solvation process, step 3, is the predominant limiting factor for the charge transfer process. Jow *et al*.[7] also reported that activation energy of Li^+ charge transfer resistance could be varied with the selection of solvents and salts.

This paper will report the studies of kinetics of practical Li-ion cells designed for high power performance using both the AC and DC impedance methods to examine and compare the limiting processes with cells of different electrolyte systems.

Experimental

Commercially available lithium iron phosphate (LFP) based 26650 Li-ion cells (acquired in 2006) with a capacity of 2.2 Ah and, Saft 3.0 Ah developmental Fat-D size lithium cobalt nickel aluminum mixed metal oxides (NCA) based high power Li-ion cells and Saft large format NCA and LFP based high power Li-ion cells, VL34P and VL25Fe[7], respectively, were used for kinetic studies. The Saft cells are of identical size with similar internal construction, anode materials, separator and electrolyte. The only notable differences are in cathodes materials. The performance and specifications of the large format VL25Fe has recently been reported by Deveney et al.[9]. The Saft high power cells used in these studies contain an electrolyte made of $LiPF_6$ in a mixture of carbonate

solvents, ester solvent and vinylene carbonate (VC) additive, which are different from conventional electrolytes made of $LiPF_6$ in mostly carbonate solvent mixtures.

AC Impedance Measurement

AC impedance of 2.2 Ah 26650 LFP Li-ion cells and Saft 3.0 Ah developmental NCA Li-ion were measured using Solartron Frequency Response Analyzer (FRA Model 1260) coupled with the Solartron Electrochemical Interface (EI Model 1287). This measurement was carried out at different temperatures and various state-of-charges (SOCs).

Pulse DC Impedance Measurement

VL34P and VL25Fe cells were used for pulse DC impedance studies. Pulse DC impedance of these cells was determined by the voltage changes under a 40 A pulse current at 100 ms and 15 s. This measurement was carried out at different temperatures and various SOCs.

Results and Discussion

The AC impedance and the DC pulse impedance measurements reveal different aspects of the kinetic process in Li-ion cells. Through AC impedance method, different electrochemical processes in a cell are interpreted using an equivalent circuit. Through DC pulse impedance method, the voltage changes at different time intervals reveal the impedance that the current encountered at, most likely, the rate limiting steps. The results will be presented and discussed in the following sections.

AC Impedance Measurement

As shown in Fig. 1, a single semi-circle is shown in the Electrochemical Impedance Spectra (EIS) of the LFP 26650 cell at –10 ^{o}C. In the same figure, instead of one semi-circle for LFP, two semi-circles appeared in the EIS for the impedance of the 3 Ah NCA cell at –10 ^{o}C or higher temperatures. At –30 and –40 ^{o}C, the two semicircles that were observed at –10 ^{o}C were merged and appeared to be one.

The set-up used in this study was not ideal for the measurement of AC impedance of low impedance high power cells such as LFP 26650 or 3 Ah NCA cells. This is mainly due to the fact that, even under low voltage perturbation, the corresponding cell current sometimes reaches beyond the measurement capability of the present instruments. The data points at high frequencies fall below x-axis in the EIS reflect the impact of the inductance coming from the spirally wound configuration the cells. Furthermore, the added capacitance coming from the extended cables for reaching the cells in the environmental chamber needs to be corrected for accurate measurement.

If assigning the diameters of either joint two-semicircles or one semicircle as Li^+ as the charge-transfer resistance, R_{ct}, which increases apparently with decreasing temperature, we can determine the activation energy of the Li^+ charge-transfer process from the slope of the log $1/R_{ct}$ versus 1/T plot. The activation energy for Li^+ charge

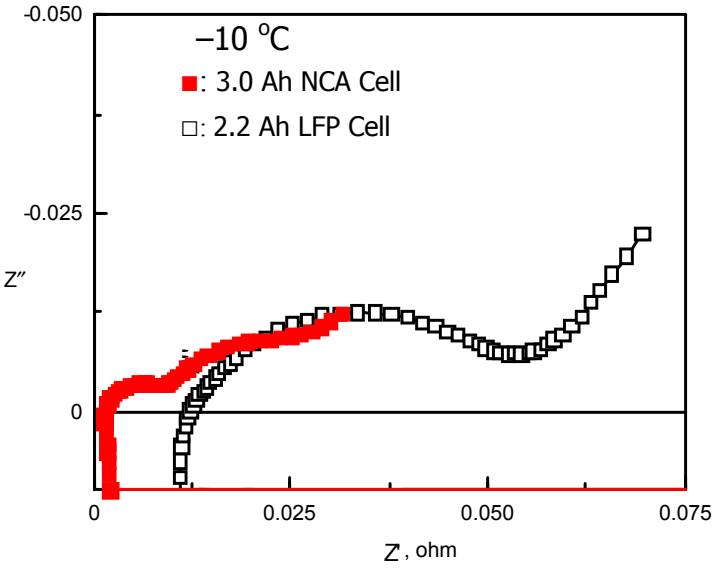

Figure 1. EIS at –10 °C for 3.0 Ah NCA cell and 2.2 Ah LFP cell.

transfer resistance obtained in both cases were in a range between 60 and 70 kJ/mol, which are very close to the value that were reported earlier[7].

Due to mainly the differences in electrolytes, we expect to see different activation energies for Li^+ charge transfer for these two different cells based on the studies by Ogumi and his group[2-6] and Jow *et al.*[7] However, these preliminary results were compromised by the limitation of the instruments and set-up. The measurement using instrumentation with higher current capability and proper set up is under way. The results will be reported elsewhere.

Pulse DC Impedance Measurement

The Pulse DC impedance, R_{DC}, of VL25Fe of 90% SOC measured under a 40 A pulse current at 100 ms and 15 sec, respectively, at different temperatures are shown in Fig. 2. It is interesting to observe that R_{DC} during discharge is about the same as that during charge at 100 ms, with discharge resistance even slightly higher than charge resistance during charge. At 15 s, R_{DC} during charge is obviously higher than that during discharge at temperatures below –10 °C.

A comparison of pulse DC impedance of NCA cell and LFP cell during charge is shown in Fig. 3. At 100 ms, R_{DC} is almost identical for NCA and LEP cells. At 15 s, R_{DC} of LFP cell becomes higher than that of NCA cell at temperatures below –20 °C. This may suggest that the diffusion of Li in LFP at low temperatures is impeding the overall charging rate considering the same anode and electrolyte were used in both cells.

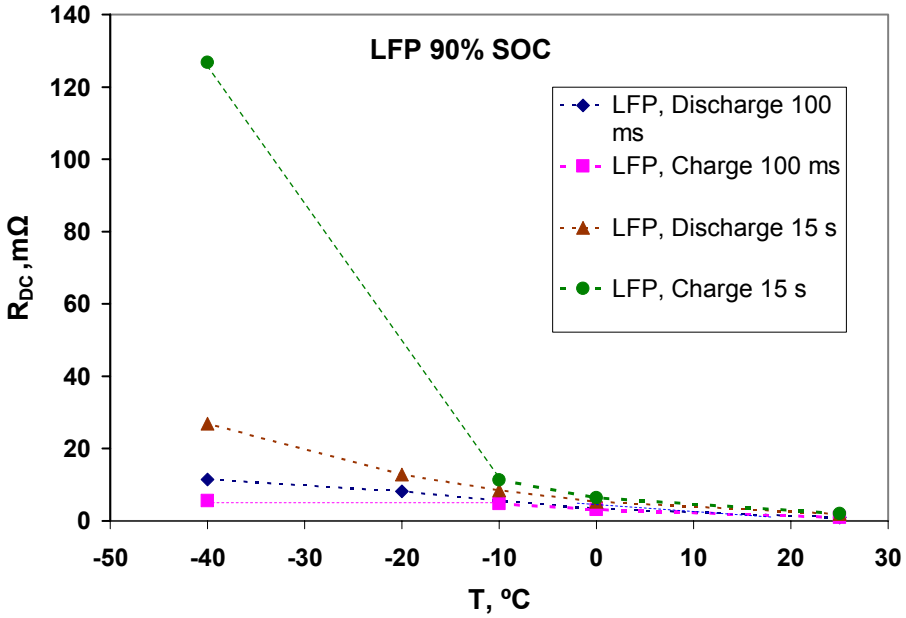

Figure 2. Pulse DC impedance during discharge and charge at various temperatures for a VL25Fe cell under 40 A pulse current measured at 100 ms and 15 s.

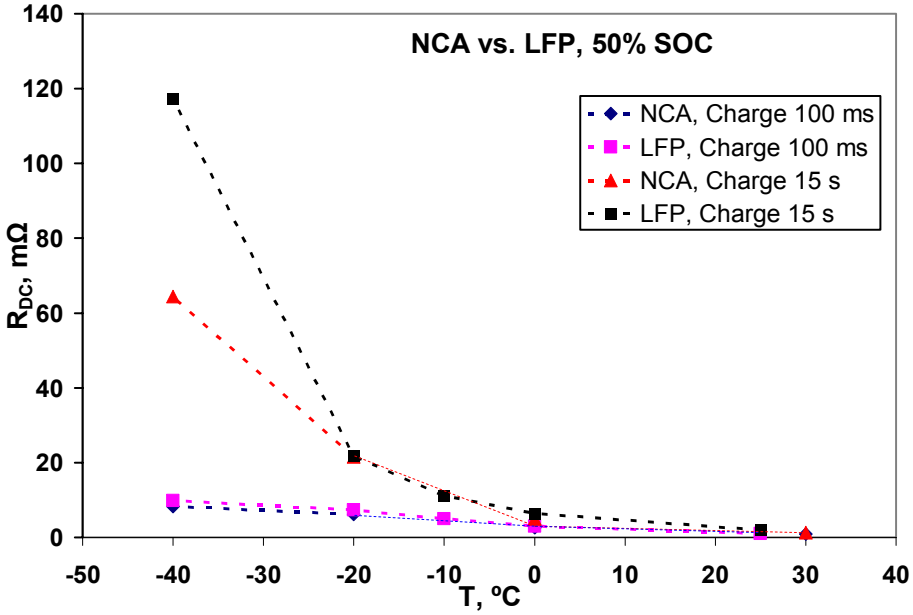

Figure 3. Pulse DC impedance during charge at various temperatures for VL34P (NCA) and VL25Fe (LFP) cells at 50% SOC under 40 A pulse current measured at 100 ms and 15 s.

We can use the slope of the log of $1/R_{DC}$ versus $1/T$ plot as the activation energy, E_a, for overall charge or discharge process. For NCA cells, as shown in Fig. 4, the activation energy for charge is higher than that for discharge at 15 s but of almost the same

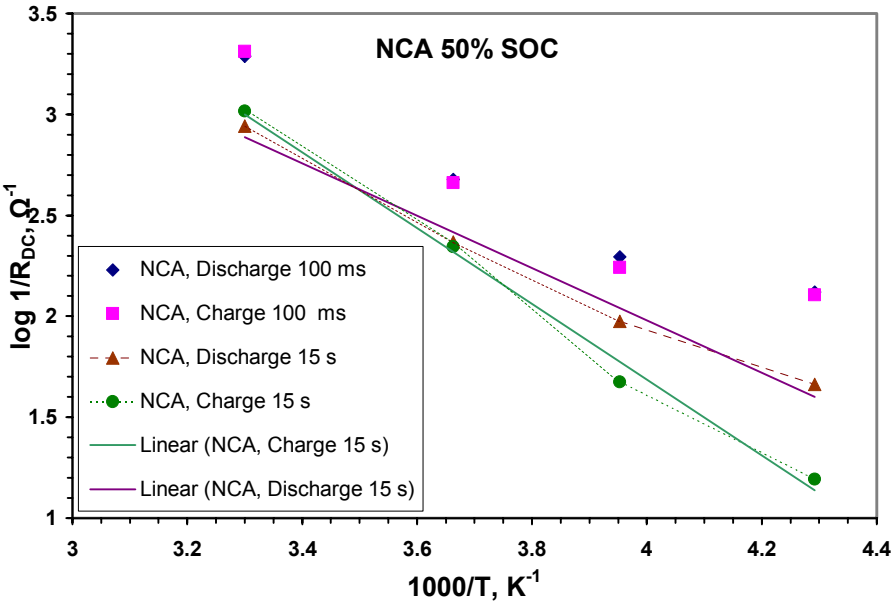

Figure 4. The plot of log ($1/R_{DC}$) versus 1/T at various temperatures for VL34P (NCA) Li-ion cell, where R_{DC}s were obtained at 100 ms and 15 s pulse periods during charge and discharge.

activation energy for both charge and discharge at 100 ms. The activation energies for charge and discharge of LFP cells at 100 ms and 15 s were also determined by the same method. These results are summarized in Table I. At 15 s, the activation energy for charge are 36 kJ/mol for NCA cells and 39 kJ/mol for LFP cells, which are about 50% higher than those for discharge, respectively. As the E_a values shown in the table, we found that the charge-discharge kinetics of LFP is just about as fast as NCA and is probably only slightly slower. At 15 s, it is apparent that charge kinetics is slower than discharge kinetics regardless of the cathode materials.

Table I Charge-Discharge Activation Energy of VL34P (NCA) and VL25Fe (LFP) Li-ion Cells at 50% SOC

E_a, kJ/mol	At 100 ms		At 15 s	
	Discharge	**Charge**	**Discharge**	**Charge**
NCA	22.78	23.74	24.89	35.99
LFP	31.01	26.04	25.77	38.67

During charge, desolvation of "Li^+" and electron transfer steps, steps 3 and 4, occur at the anode. During discharge, desolvation of "Li^+" and electron transfer steps occur at the cathode. Therefore, the question is what makes the charge kinetics slower than the discharge kinetics. Let's assume that the kinetics is slowed at the anode during charge at 15 s. It is reasonable to believe that this is not caused by the desolvation step alone. How fast Li^+ is moving across the SEI may impact the "Li^+" desolvation rate. The electron transfer step, which involves simultaneously Li^+ accepting electron from the electrode and Li intercalation into the host materials, and the diffusion of Li in anode need to be considered too.

It is also possible that the kinetics is slowed at the cathode. Then, we need to consider that the SEI-affected de-intercalation rate and Li diffusion rate in cathode are

slowed assuming that the Li^+ solvation rate is faster. If desolvation is the limiting step, then we would believe that step is significantly affected by the SEI, intercalation and diffusion in the anode.

Conclusions

Preliminary AC impedance studies were made on commercial 26650 LFP cells and 3.0 Ah NCA Fat D high power cells with different electrolytes and cathodes. Similar activation energies were found for both cells. The results might be compromised by the difficulties involved in measuring very low resistance cells. The pulse DC impedance at 15 s data indicates that the charge kinetics are slower than the discharge kinetics for both VL34P (NCA) and VL25Fe (LFP) cells, which have the same physical configuration, anode and electrolyte except cathodes. At 100 ms, the charge-discharge kinetics is almost the same. These results lead us to believe that, if desolvation is the limiting step, the desolvation is significantly affected by SEI, intercalation into anode and diffusion in the anode.

Acknowledgments

The authors wish to thank the Office of Vehicle Technologies of the Department of Energy for partial financial support and Dr. Jeffrey Read of ARL for helpful discussion.

References

1. T. R. Jow and C. C. Liang, *J. Electrochem. Soc*., **130**, 737 (1983).
2. T. Abe, N. Kawabata, Y. Mizutani, .M. Inaba, and Z. Ogumi, *J. Electrochem. Soc.*, **150**(3), A257 (2003).
3. T. Abe, H. Fukuda, Y. Iriyama, and Z. Ogumi, *J. Electrochem. Soc.*, **151**(8), A1120 (2004).
4. T. Abe, F. Sagane, M. Ohtsuka, Y. Iriyama, and Z. Ogumi, *J. Electrochem. Soc.*, **152**(11), A2151 (2005).
5. K. Abe, T. Hattori, K. Kawabe, Y. Ushigoe, H. Yoshitake, *J. Electrochem. Soc.*, **154**(8), A810 (2007).
6. Y. Ishihara, Y. Yamada, Y. Iriyama, T. Abe, Z. Ogumi, 2008 IMLB, Abstract #105, Tianjin, China, June 22-28, 2008.
7. T. R. Jow, S. S. Zhang, K. Xu, J. L. Allen, *ECS Transactions*, **3**(27), 51-58 (2007).
8. http://www.saftbatteries.com/
9. B. Deveney, K. Nechev, T. R. Jow, K. Xu**,** *Proc. of 43rd Power Sources Conference*, p. 457, Philadelphia, PA, 7-10 July 2008.